Advances in Materials Research, *Vol. 8, No. 3 (2019) 155-177*
DOI: https://doi.org/10.12989/amr.2019.8.3.155

Static analysis of functionally graded sandwich plates with porosities

Ahmed Keddouri [1,2], Lazreg Hadji [*3,4] and Abdelouahed Tounsi [2]

[1] *Department of Earth Sciences and Universe, Ziane Achour University, BP 3117, 17000 Djelfa, Algeria*
[2] *Material and Hydrology Laboratory, University of Sidi Bel Abbes 22000, Algeria*
[3] *Department of Mechanical Engineering, Ibn Khaldoun University, BP 78 Zaaroura, 14000 Tiaret, Algeria*
[4] *Laboratory of Geomatics and Sustainable Development, Ibn Khaldoun University of Tiaret, Algeria*

(*Received August 21, 2019, Revised October 26, 2019, Accepted November 1, 2019*)

Abstract. In this paper, a new displacement based high-order shear deformation theory is introduced for the static response of functionally graded sandwich plate with new definition of porosity distribution taking into account composition and the scheme of the sandwich plate. Unlike any other theory, the number of unknown functions involved is only four, as against five in case of other shear deformation theories. The theory presented is variationally consistent, has strong similarity with classical plate theory in many aspects, does not require shear correction factor, and gives rise to transverse shear stress variation such that the transverse shear stresses vary parabolically across the thickness satisfying shear stress free surface conditions. Material properties of FGM layers are assumed to vary continuously across the plate thickness according to either power-law or sigmoid function in terms of the volume fractions of the constituents. The face layers are considered to be FG across each face thickness while the core is made of a ceramic homogeneous layer. Governing equations are derived from the principle of virtual displacements. The closed-form solution of a simply supported rectangular plate subjected to sinusoidal loading has been obtained by using the Navier method. Numerical results are presented to show the effect of the material distribution, the sandwich plate geometry and the porosity on the deflections and stresses of FG sandwich plates. The validity of the present theory is investigated by comparing some of the present results with other published results.

Keywords: functionally graded materials; sandwich plates; refined plate theory; bending; Navier solution; porosity

1. Introduction

Functionally Graded Materials (FGMs) are a class of composites that have received great attention in many modern engineering applications such as military, aerospace, nuclear energy, biomedical, automotive, civil engineering and marine. Due to its high resistance to temperature shocks and no interface problems through the layer interfaces, the researchers have extensively examined the static, vibration and buckling responses of these structures during the last decade (Kadoli *et al*. 2008, Simsek 2010, Menaa *et al*. 2012).

In recent years, and with the developments in manufacturing methods, the FGMs are

*Corresponding author, Ph.D., E-mail: had_laz@yahoo.fr

http://www.techno-press.org/?journal=amr&subpage=5 ISSN: 2234-0912 (Print), 2234-179X (Online)

considered in the industry of the sandwich structures because of the gradual variation of material properties at the interfaces between the face layers and the core. Because of the importance and extensive technical applications of the FGM sandwich structures, understanding of their responses becomes an important task. Several researches have been performed to analyze the bending behavior of FG sandwich beams and plates. Zenkour and Alghamdi (2010) examined thermoelastic bending of FG sandwich plates based on the higher-order shear deformation theories (HSDT). Tounsi *et al*. (2013) developed a refined trigonometric shear deformation theory for thermoelastic bending of functionally graded sandwich plates. Xuan *et al*. (2013) analyze the isogeometric finite element of composite sandwich plates using a higher order shear deformation theory. Vo *et al*. (2015) developed the static behaviour of functionally graded sandwich beams using a quasi-3D theory. Simsek and Al-shujairi (2017) studied the static, free and forced vibration of functionally graded (FG) sandwich beams excited by two successive moving harmonic loads. Benhenni *et al*. (2018) analyze the dynamic for anti-symmetric cross-ply and angle-ply laminates for simply supported thick hybrid rectangular plates. Karamanlı (2017) investigated the bending behaviour of two directional functionally graded sandwich beams by using a quasi-3d shear deformation theory. Shashank and Pradyumna (2018) used a higher-order layerwise theory for functionally graded sandwich plates. Zarga *et al*. (2019) used a simple quasi-3D shear deformation theory for the thermomechanical bending study for functionally graded sandwich plates. Meksi *et al*. (2019) developed an analytical solution for bending, buckling and vibration responses of FGM sandwich plates. Hellal *et al*. (2019), used a simple higher shear deformation theory for the dynamic and stability analysis of functionally graded material sandwich plates in hygro-thermal environment. Akbaş (2015a) developed the wave propagation of a functionally graded beam in thermal environments. Akbaş (2015b) studied the post-buckling analysis of axially functionally graded three-dimensional beams. Akbaş (2017a) analyze the free vibration of edge cracked functionally graded microscale beams based on the modified couple stress theory. Akbaş (2018a) investigated the nonlinear thermal displacements of laminated composite beams. Akbaş (2018b) studied the forced vibration analysis of cracked nanobeams. Akbaş (2018c) analyze the forced vibration of cracked functionally graded microbeams. Safa *et al*. (2019) analyze the thermal vibration of FGM beams using an efficient shear deformation beam theory. Sahouane *et al*. (2019) developed a numerical analysis for free vibration of functionally graded beams using an original HSDBT. Zouatnia and Hadji (2019) studied the effect of the micromechanical models on the bending of FGM beam using a new hyperbolic shear deformation theory.

In addition, in FGM fabrication, micro voids or porosities can occur within the materials during the process of sintering. This is because of the large difference in solidification temperatures between material constituents (Zhu *et al*. 2001). Wattanasakulpong *et al*. (2012) also gave the discussion on porosities happening inside FGM samples made by a multistep sequential infiltration technique. Therefore, it is important to take into account the porosity effect when designing FGM structures subjected to dynamic loadings. Recently, Wattanasakulpong and Ungbhakorn (2014) studied linear and nonlinear vibration problems of elastically end restrained FG beams having porosities. In the same way Ait Yahia *et al*. (2015) investigated the wave propagation of an infinite FG plate having porosities by using various simple higher-order shear deformation theories. Akbaş (2017b) analyze the thermal effects on the vibration of functionally graded deep beams with porosity. Bourada *et al*. (2019) investigated the dynamic of porous functionally graded beam using a sinusoidal shear deformation theory. Recently Daikh and Zenkour (2019) studied the effect of porosity on the bending analysis of various functionally graded sandwich plates.

As far as we know, there has been no investigation on bending of the FGM sandwich plates

with porosities using the four-variable refined plate theory (RPT). In the present study, a new porosities distribution is proposed for bending analysis of new model of functionally graded material (FGM) sandwich plates. Material properties of FGM layers are assumed to vary continuously across the plate thickness according to either power-law or sigmoid function in terms of the volume fractions of the constituents. The four-variable refined plate theory is proposed to derive the field equations of the FG sandwich plates with simply-supported edge conditions. The most interesting feature of this theory is that it does not require the shear correction factor and satisfies equilibrium conditions at the top and bottom faces of the sandwich plate. The Navier solution is used to obtain the closed form solutions for simply supported FGM sandwich plates. Numerical examples are presented to verify the accuracy of the present theory. Numerical results are presented to show the effect of the material distribution, the sandwich plate geometry and the porosity on the deflections and stresses of FG sandwich plates.

2. FGM sandwich plates

Consider the case of a uniform thickness, rectangular FGM sandwich plate composed of three microscopically heterogeneous layers (metal-ceramic, ceramic, ceramic-metal), with reference to rectangular coordinates (x, y, z) as depicted in Fig. 1. The top and bottom faces of the plate are at z = ±h/2, and the edges of the plate are parallel to axes x and y. The sandwich plate is composed of three elastic layers, namely ‘‘Layer 1”, ‘‘Layer 2,’’ and ‘‘Layer 3’’ from the uppermost surface to the lowest surface of the plate. The vertical ordinates of the bottom, the two interfaces, and the top are denoted by $h_1 = -h/2,\ h_2,\ h_3$, and $h_4 = +h/2$, respectively. Two types of sandwich plates are used: power-law FG sandwich plates P-FGM and sigmoid FG sandwich plates S-FGM.

2.1 Power-law FG sandwich plate

The sandwich plate is made of three layers, an isotropic core and two power-law FG layers. The face layers are graded from metal to ceramic while the core layer is made of ceramic. The volume fraction $V^{(n)}$ of layer n $(n = 1,2,3)$, varies according to the following power-law function across the plate thickness

$$V^{(1)}(z) = \left(\frac{z - h_1}{h_2 - h_1}\right)^p, \qquad h_1 \le z \le h_2 \tag{1a}$$

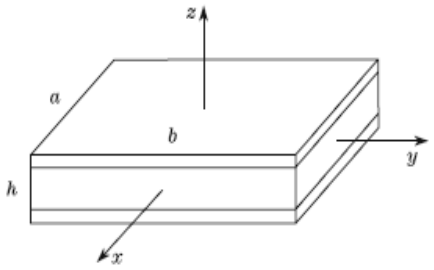

Fig. 1 Geometry of the rectangular FGM sandwich plate with uniform thickness in rectangular Cartesian coordinates

$$V^{(2)}(z) = 1, \qquad h_2 \le z \le h_3 \tag{1b}$$

$$V^{(3)}(z) = \left(\frac{z - h_4}{h_3 - h_4}\right)^p, \qquad h_3 \le z \le h_4 \tag{1c}$$

Where p denotes volume fraction index. When $p = 0$ we return to the fully homogeneous ceramic plate.

2.2 Sigmoid FG sandwich plate

Here, the volume fraction varies according to a sigmoid function through-the-thickness as follows

$$V_1^{(1)}(z) = \frac{1}{2}\left(\frac{z - h_1}{h_m - h_1}\right)^p, \qquad h_1 \le z \le h_m \tag{2a}$$

$$V_2^{(1)}(z) = 1 - \frac{1}{2}\left(\frac{z - h_2}{h_m - h_2}\right)^p, \qquad h_m \le z \le h_2 \tag{2b}$$

$$V^{(2)}(z) = 1, \qquad h_2 \le z \le h_3 \tag{2c}$$

$$V_1^{(3)}(z) = 1 - \frac{1}{2}\left(\frac{z - h_3}{h_n - h_3}\right)^p, \qquad h_3 \le z \le h_n \tag{2d}$$

$$V_2^{(1)}(z) = \frac{1}{2}\left(\frac{z - h_4}{h_n - h_4}\right)^p, \qquad h_n \le z \le h_4 \tag{2e}$$

where $h_m = (h_1 + h_2)/2$ and $h_m = (h_3 + h_4)/2$ denotes the middle surface positions of the bottom and the top layer, respectively.

3. Porosity-dependent FG sandwich plates

Effective material properties of FGMs are influenced by various factors such as high temperature, humidity and porosity. In this paper, the porosity effect is investigated. Numerous models of porosities distribution have been proposed by the researchers to compute the effective material properties of porous FGM plate (Wattanasakulpong and Ungbhakorn 2014). In this paper, for the first time, the porosities are distributed independently in each FGM layer of sandwich. Four models of porosity are used.

3.1 Imperfect FGM with even porosities (Imperfect I)

Let us assume that the FG sandwich plate is fabricated of a mixture of metal and ceramic. The influence of porosities, which may exist inside the materials of FGM layers during the production,

is included. The porosities uniformly distributed over the FGM sandwich layers, whereas the core layer is perfect (nonporous) and made of ceramic. By using the rule of mixture, the effective material properties $P^{(n)}$ of layer $n\ (n = 1,2,3)$ with evenly distributed porosities (imperfect I), are stated as

$$\begin{aligned} P^{(1)}(z) &= (P_c - P_m)V^{(1)}(z) + P_m - \frac{\alpha}{2}(P_c + P_m) \\ P^{(2)}(z) &= (P_c - P_m)V^{(2)}(z) + P_m \\ P^{(3)}(z) &= (P_c - P_m)V^{(3)}(z) + P_m - \frac{\alpha}{2}(P_c + P_m) \end{aligned} \tag{3}$$

where α denotes the porosity coefficient $(\alpha \prec\prec 1)$. P_c and P_m are the corresponding properties of the ceramic and metal, respectively.

3.2 Imperfect FGM with uneven porosities (Imperfect II)

Here, the porosities may spread functionally during the thickness direction of the FGM sandwich as follow

$$\begin{aligned} P^{(1)}(z) &= (P_c - P_m)V^{(1)}(z) + P_m - \frac{\alpha}{2}(P_c + P_m)\left[1 - \frac{|2z - h_1 - h_2|}{h_2 - h_1}\right] \\ P^{(2)}(z) &= (P_c - P_m)V^{(2)}(z) + P_m \\ P^{(3)}(z) &= (P_c - P_m)V^{(3)}(z) + P_m - \frac{\alpha}{2}(P_c + P_m)\left[1 - \frac{|2z - h_4 - h_3|}{h_4 - h_3}\right] \end{aligned} \tag{4}$$

3.3 Imperfect FGM with logarithmic-uneven porosities (Imperfect III)

Another uneven model based on a logarithmic function can be expressed as

$$\begin{aligned} P^{(1)}(z) &= (P_c - P_m)V^{(1)}(z) + P_m - log\left(1 + \frac{\alpha}{2}\right)(P_c + P_m)\left[1 - \frac{|2z - h_1 - h_2|}{h_2 - h_1}\right] \\ P^{(2)}(z) &= (P_c - P_m)V^{(2)}(z) + P_m \\ P^{(3)}(z) &= (P_c - P_m)V^{(3)}(z) + P_m - log\left(1 + \frac{\alpha}{2}\right)(P_c + P_m)\left[1 - \frac{|2z - h_4 - h_3|}{h_4 - h_3}\right] \end{aligned} \tag{5}$$

3.4 Imperfect FGM with linear-uneven porosities (Imperfect IV)

The density of porosity is low at the outer surfaces of the sandwich and high at the two interfaces positions, and change across the FGM layers with linear function as

$$\begin{aligned} P^{(1)}(z) &= (P_c - P_m)V^{(1)}(z) + P_m - \frac{\alpha}{2}(P_c + P_m)\left[1 - \frac{z - h_2}{h_1 - h_2}\right] \\ P^{(2)}(z) &= (P_c - P_m)V^{(2)}(z) + P_m \\ P^{(3)}(z) &= (P_c - P_m)V^{(3)}(z) + P_m - \frac{\alpha}{2}(P_c + P_m)\left[\frac{z - h_4}{h_3 - h_4}\right] \end{aligned} \tag{6}$$

4. Mathematical formulation

4.1 Basic assumptions

The assumptions of the present theory are as follows:

- The displacements are small in comparison with the plate thickness. Therefore, the strains involved are infinitesimal.
- The transverse displacement $w$includes two components of bending w_b, and shear w_s. These components are functions of coordinates x, y and time t only.

$$w(x,y,z,t) = w_b(x,y,t) + w_s(x,y,t) \tag{7}$$

The transverse normal stress σ_z is negligible in comparison with in-plane stresses σ_x and σ_y.
- The axial displacement u in x-direction and v in the y-direction, consists of extension, bending, and shear components.

$$u = u_0 + u_b + u_s, \qquad v = v_0 + v_b + v_s \tag{8}$$

- The bending component u_b and v_b are assumed to be similar to the displacements given by the classical plate theory. Therefore, the expression for u_b and v_b can be given as

$$u_b = -z\frac{\partial w_b}{\partial x}, \qquad v_b = -z\frac{\partial w_b}{\partial y} \tag{9}$$

- The shear components u_s and v_s gives rise, in conjunction with w_s, to the hyperbolic variation of shear strains γ_{xz}, γ_{yz} and hence to shear stresses τ_{xz}, τ_{yz} through the thickness of the plate in such a way that shear stresses τ_{xz}, τ_{yz} are zero at the top and bottom faces of the plate. Consequently, the expression for u_s and v_s can be given as

$$u_s = -f(z)\frac{\partial w_s}{\partial x}, \qquad v_s = -f(z)\frac{\partial w_s}{\partial y} \tag{10}$$

where

$$f(z) = -\frac{z}{4} + \frac{5z^3}{3h^2} \tag{11}$$

4.2 Kinematics and constitutive equations

Based on the assumptions made in the preceding section, the displacement field can be obtained using Eqs. (7)-(11) as

$$\begin{aligned} u(x,y,z) &= u_0(x,y,t) - z\frac{\partial w_b}{\partial x} - f(z)\frac{\partial w_s}{\partial x} \\ v(x,y,z) &= v_0(x,y,t) - z\frac{\partial w_b}{\partial y} - f(z)\frac{\partial w_s}{\partial y} \end{aligned} \tag{12}$$

$$w(x,y,z) = w_b(x,y) + w_s(x,y) \tag{12}$$

The strains associated with the displacements in Eq. (12) are

$$\begin{aligned} \varepsilon_x &= \varepsilon_x^0 + z\,k_x^b + f(z)\,k_x^s \\ \varepsilon_y &= \varepsilon_y^0 + z\,k_y^b + f(z)\,k_y^s \\ \gamma_{yz} &= g(z)\,\gamma_{yz}^s \\ \gamma_{xz} &= g(z)\,\gamma_{xz}^s \\ \varepsilon_z &= 0 \end{aligned} \tag{13}$$

where

$$\begin{aligned} \varepsilon_x^0 &= \frac{\partial u_0}{\partial x}, \qquad k_x^b = -\frac{\partial^2 w_b}{\partial x^2}, \qquad k_x^s = -\frac{\partial^2 w_s}{\partial x^2}, \\ \varepsilon_y^0 &= \frac{\partial v_0}{\partial x}, \qquad k_y^b = -\frac{\partial^2 w_b}{\partial y^2}, \qquad k_y^s = -\frac{\partial^2 w_s}{\partial y^2}, \\ \gamma_{yz}^s &= -\frac{\partial w_s}{\partial x}, \qquad \gamma_{xz}^s = \frac{\partial w_s}{\partial x}, \\ g(z) &= 1 - f'(z), \qquad f'(z) = \frac{df(z)}{dz} \end{aligned} \tag{14}$$

For elastic and isotropic FGMs, the constitutive relations can be written as

$$\begin{Bmatrix} \sigma_x \\ \sigma_y \\ \tau_{yz} \\ \tau_{xz} \\ \tau_{xy} \end{Bmatrix}^{(n)} = \begin{bmatrix} Q_{11} & Q_{12} & 0 & 0 & 0 \\ Q_{12} & Q_{22} & 0 & 0 & 0 \\ 0 & 0 & Q_{44} & 0 & 0 \\ 0 & 0 & 0 & Q_{55} & 0 \\ 0 & 0 & 0 & 0 & Q_{66} \end{bmatrix}^{(n)} \begin{Bmatrix} \varepsilon_x \\ \varepsilon_y \\ \gamma_{yz} \\ \gamma_{xz} \\ \gamma_{xy} \end{Bmatrix}^{(n)} \tag{15}$$

where

$$Q_{11}(z) = \frac{E(z)}{(1-\nu^2)}, \qquad Q_{12}(z) = \nu Q_{11}(z) \tag{16}$$

and

$$Q_{44}(z) = Q_{55}(z) = Q_{66}(z) = \frac{E(z)}{2(1+\nu)} \tag{17}$$

4.3 Governing equations

The governing equations of equilibrium can be derived by using the principle of virtual displacements. The principle of virtual work in the present case yields

$$\begin{aligned} &\int_{-h/2}^{h/2} \int_{\Omega} \begin{bmatrix} \sigma_x \delta\varepsilon_x + \sigma_y \delta\varepsilon_y + \tau_{xy}\delta\gamma_{xy} \\ +\tau_{xz}\delta\gamma_{xz} + \tau_{yz}\delta\gamma_{yz} \end{bmatrix} d\Omega dz \\ &- \int_{\Omega} q(x,y)\,\delta w d\Omega = 0 \end{aligned} \tag{18}$$

where Ω is the top surface and $q(x,y)$ is the applied transverse load.

Substituting Eqs. (13) and (15) into Eq. (18) and integrating through the thickness of the plate, Eq. (18) can be rewritten as

$$\int_{\Omega}\begin{bmatrix} N_x\delta\varepsilon_x^0+N_y\delta\varepsilon_y^0+N_{xy}\delta\gamma_{xy}^0+M_x^b\delta k_x^b \\ +M_y^b\delta k_y^b+M_{xy}^b\delta k_{xy}^b+M_x^s\delta k_x^s+M_y^s\delta k_y^s \\ +M_{xy}^s\delta k_{xy}^s+S_{yz}^s\delta\gamma_{yz}^s+S_{xz}^s\delta\gamma_{xz}^s \end{bmatrix}d\Omega-\int_{\Omega}q\delta w d\Omega=0, \tag{19}$$

where

$$\begin{Bmatrix} N_x, & N_y, & N_{xy} \\ M_x^b, & M_y^b, & M_{xy}^b \\ M_x^s, & M_y^s, & M_{xy}^s \end{Bmatrix}=\sum_{n=1}^{3}\int_{h_n}^{h_{n+1}}\left(\sigma_x,\sigma_y,\tau_{xy}\right)^{(n)}\begin{Bmatrix}1\\ z\\ f(z)\end{Bmatrix}dz \tag{20a}$$

and

$$\left(S_{xz}^s,S_{yz}^s\right)=\sum_{n=1}^{3}\int_{h_n}^{h_{n+1}}\left(\tau_{xz},\tau_{yz}\right)^{(n)}g(z)dz \tag{20b}$$

where h_{n+1} and $h_n$are the top and bottom z-coordinates of the nth layer.

The governing equations of equilibrium can be derived from Eq. (18) by integrating the displacement gradients by parts and setting the coefficients zero $\delta u0$, $\delta v0$, δwb, and δws separately. Thus one can obtain the equilibrium equations associated with the present refined shear deformation plate theory

$$\begin{aligned} &\delta\, u_0\colon \ \frac{\partial N_x}{\partial x}+\frac{\partial N_y}{\partial y}=0 \\ &\delta\, v_0\colon \ \frac{\partial N_{xy}}{\partial x}+\frac{\partial N_y}{\partial y}=0 \\ &\delta\, w_b\colon \ \frac{\partial^2 M_x^b}{dx^2}+2\frac{\partial^2 M_{xy}^b}{\partial x^2\partial y^2}+\frac{\partial^2 M_y^b}{dy^2}+q=0 \\ &\delta\, w_s\colon \ \frac{\partial^2 M_x^s}{dx^2}+2\frac{\partial^2 M_{xy}^s}{\partial x^2\partial y^2}+\frac{\partial^2 M_y^s}{dy^2}+\frac{\partial S_{xz}^s}{\partial x}+\frac{\partial S_{yz}^s}{\partial y}+q=0 \end{aligned} \tag{21}$$

Substituting Eq. (15) into Eq. (20) and integrating through the thickness of the plate, the stress resultants are given as

$$\begin{Bmatrix} N \\ M^b \\ M^s \end{Bmatrix}=\begin{bmatrix} A & B & B^s \\ B & D & D^s \\ B^s & D^s & H^s \end{bmatrix}\begin{Bmatrix} \varepsilon \\ k^b \\ k^s \end{Bmatrix}, \qquad S=A^s\gamma \tag{22}$$

where

$$N=\left\{N_x,N_y,N_{xy}\right\}^t, \qquad M^b=\left\{M_x^b,M_y^b,M_{xy}^b\right\}^t, \qquad M^s=\left\{M_x^s,M_y^s,M_{xy}^s\right\}^t, \tag{23a}$$

$$\varepsilon=\left\{\varepsilon_x^0,\varepsilon_y^0,\gamma_{xy}^0\right\}^t, \qquad k^b=\left\{k_x^b,k_y^b,k_{xy}^b\right\}^t, \qquad k^s=\left\{k_x^s,k_y^s,k_{xy}^s\right\}^t, \tag{23b}$$

$$A=\begin{bmatrix}A_{11} & A_{12} & 0\\ A_{12} & A_{22} & 0\\ 0 & 0 & A_{66}\end{bmatrix},\qquad A=\begin{bmatrix}B_{11} & B_{12} & 0\\ B_{12} & B_{22} & 0\\ 0 & 0 & B_{66}\end{bmatrix},\qquad D=\begin{bmatrix}D_{11} & D_{12} & 0\\ D_{12} & D_{22} & 0\\ 0 & 0 & D_{66}\end{bmatrix}, \tag{23c}$$

$$B^s=\begin{bmatrix}B^s_{11} & B^s_{12} & 0\\ B^s_{12} & B^s_{22} & 0\\ 0 & 0 & B^s_{66}\end{bmatrix},\qquad D^s=\begin{bmatrix}D^s_{11} & D^s_{12} & 0\\ D^s_{12} & D^s_{22} & 0\\ 0 & 0 & D^s_{66}\end{bmatrix},\qquad H^s=\begin{bmatrix}H^s_{11} & H^s_{12} & 0\\ H^s_{12} & H^s_{22} & 0\\ 0 & 0 & H^s_{66}\end{bmatrix}, \tag{23d}$$

$$S=\left\{S^s_{xz},S^s_{yz}\right\}^t,\qquad \gamma=\left\{\gamma_{xz},\gamma_{yz}\right\}^t,\qquad A^s=\begin{bmatrix}A^s_{44} & 0\\ 0 & A^s_{55}\end{bmatrix}, \tag{23e}$$

The stiffness coefficients A_{ij}, B_{ij} and D_{ij}, etc., are defined as

$$\begin{Bmatrix}A_{11} & B_{11} & D_{11} & B^s_{11} & D^s_{11} & H^s_{11}\\ A_{12} & B_{12} & D_{12} & B^s_{12} & D^s_{12} & H^s_{12}\\ A_{66} & B_{66} & D_{66} & B^s_{66} & D^s_{66} & H^s_{66}\end{Bmatrix} = \sum_{n=1}^{3}\int_{\hbar_n}^{\hbar_{n+1}} Q_{11}^{(n)}(1,z,z^2,f(z),z\,f(z),f^2(z))\begin{Bmatrix}1\\ \nu^{(n)}\\ \dfrac{1-\nu^{(n)}}{2}\end{Bmatrix}dz \tag{24a}$$

$$(A_{22},B_{22},D_{22},B^s_{22},D^s_{22},H^s_{22})=(A_{11},B_{11},D_{11},B^s_{11},D^s_{11},H^s_{11}) \tag{24b}$$

$$A^s_{44}=A^s_{55}=\sum_{n=1}^{3}\int_{\hbar_n}^{\hbar_{n+1}}\frac{E(z)}{2(1+\nu)}[g(z)]^2dz \tag{24c}$$

By substituting Eq. (22) into Eq. (21), the equations of motion can be expressed in terms of displacements (u_0, v_0, w_b, w_s) as

$$\begin{aligned}&A_{11}\frac{\partial^2u_0}{\partial x^2}+A_{66}\frac{\partial^2u_0}{\partial y^2}+(A_{12}+A_{66})\frac{\partial^2v_0}{\partial x\partial y}B_{11}\frac{\partial^3w_b}{\partial x^3}-(B_{12}+2B_{66})\frac{\partial^3w_b}{\partial x\partial y^2}\\ &-(B^s_{12}+2B^s_{66})\frac{\partial^3w_s}{\partial x\partial y^2}-B^s_{11}\frac{\partial^3w_s}{\partial x^3}=0\end{aligned} \tag{25a}$$

$$\begin{aligned}&A_{22}\frac{\partial^2v_0}{\partial y^2}+A_{66}\frac{\partial^2v_0}{\partial x^2}+(A_{12}+A_{66})\frac{\partial^2u_0}{\partial x\partial y}\\ &-\mathrm{B}_{22}\frac{\partial^3w_b}{\partial y^3}-(B^s_{12}+2B^s_{66})\frac{\partial^3w_s}{\partial x^2\partial y}-B^s_{22}\frac{\partial^3w_s}{\partial y^3}=0\end{aligned} \tag{25b}$$

$$B_{11}\frac{\partial^3u_0}{\partial x^3}+(B_{12}+2B_{66})\frac{\partial^3u_0}{\partial xy^2}+(B_{12}+2B_{66})\frac{\partial^3v_0}{\partial x^2y}+B_{22}\frac{\partial^3v_0}{\partial y^3} \tag{25c}$$

$$-D_{11}\frac{\partial^4 w_b}{\partial x^4}-2(D_{12}+2D_{66})\frac{\partial^4 w_b}{\partial x^2\partial y^2}-D_{22}\frac{\partial^4 w_b}{\partial y^4}-D_{11}^s\frac{\partial^4 w_s}{\partial x^4}$$
$$-2(D_{12}^s+2D_{66}^s)\frac{\partial^4 w_s}{\partial x^2\partial y^2}-D_{22}^s\frac{\partial^4 w_s}{\partial y^4}+q=0 \tag{25c}$$

$$B_{11}^s\frac{\partial^3 u_0}{\partial x^3}+(B_{12}^s+2B_{66}^s)\frac{\partial^3 u_0}{\partial x\partial y^2}+(B_{12}^s+2B_{66}^s)\frac{\partial^3 v_0}{\partial x^2\partial y}+B_{22}^s\frac{\partial^3 v_0}{\partial y^3}$$
$$-D_{11}^s\frac{\partial^4 w_b}{\partial x^4}-2(D_{12}^s+2D_{66}^s)\frac{\partial^4 w_b}{\partial x^2\partial y^2}-D_{22}^s\frac{\partial^4 w_b}{\partial y^4}-H_{11}^s\frac{\partial^4 w_s}{\partial x^4} \tag{25d}$$
$$-2(H_{12}^s+2H_{66}^s)\frac{\partial^4 w_s}{\partial x^2\partial y^2}-H_{22}^s\frac{\partial^4 w_s}{\partial y^4}+A_{55}^s\frac{\partial^2 w_s}{\partial x^2}+A_{44}^s\frac{\partial^2 w_s}{\partial y^2}+q=0$$

4.4 Navier solution for simply supported rectangular sandwich plates

Rectangular plates are generally classified according to the type of support used. Here, we are concerned with the exact solutions of Eqs. (25) for a simply supported FG sandwich plate. Based on the Navier approach, the solutions are assumed as

$$\begin{Bmatrix} u_0 \\ v_0 \\ w_b \\ w_s \end{Bmatrix}=\sum_{m=1}^{\infty}\sum_{n=1}^{\infty}\begin{Bmatrix} U_{mn}\,cos(\lambda x)\,sin(\mu y) \\ V_{mn}\,sin(\lambda x)\,cos(\mu y) \\ W_{bmn}\,sin(\lambda x)\,sin(\mu y) \\ W_{smn}\,sin(\lambda x)\,sin(\mu y) \end{Bmatrix} \tag{26}$$

where U_{mn}, V_{mn}, W_{bmn} and W_{smn} are arbitrary parameters to be determined, and $\lambda=m\pi/a$ and $\mu=n\pi/b$. The transverse load q is also expanded in the double-Fourier sine series as

$$q(x,y)=\sum_{m=1}^{\infty}\sum_{n=1}^{\infty}q_{mn}\,sin(\lambda x)\,sin(\mu y) \tag{27}$$

For the case of a sinusoidally distributed load, we have

$$m=n=1 \text{ and } q_{11}=q_0 \tag{28}$$

where q_0 represents the intensity of the load at the plate centre.

Substituting Eqs. (26) and (27) into Eq. (25), the analytical solutions can be obtained from

$$\begin{bmatrix} a_{11} & a_{12} & a_{13} & a_{14} \\ a_{12} & a_{22} & a_{23} & a_{24} \\ a_{13} & a_{23} & a_{33} & a_{34} \\ a_{14} & a_{24} & a_{34} & a_{44} \end{bmatrix}\begin{Bmatrix} U_{mn} \\ V_{mn} \\ W_{bmn} \\ W_{smn} \end{Bmatrix}=\begin{Bmatrix} 0 \\ 0 \\ q_{mn} \\ q_{mn} \end{Bmatrix} \tag{29}$$

in which

$$
\begin{aligned}
a_{11} &= A_{11}\lambda^2 + A_{66}\mu^2 \\
a_{12} &= \lambda\,\mu\,(A_{12} + A_{66}) \\
a_{13} &= -\lambda\,[B_{11}\lambda^2 + (B_{12} + 2B_{66})\mu^2] \\
a_{14} &= -\lambda\,[B_{11}^s\lambda^2 + (B_{12}^s + 2B_{66}^s)\mu^2] \\
a_{22} &= A_{66}\lambda^2 + A_{22}\mu^2 \\
a_{23} &= -\mu\,[(B_{12} + 2B_{66})\lambda^2 + B_{22}\mu^2] \\
a_{24} &= -\mu\,[(B_{12}^s + 2B_{66}^s)\lambda^2 + B_{22}^s\mu^2] \\
a_{33} &= D_{11}\lambda^4 + 2(D_{12} + 2D_{66})\lambda^2\mu^2 + D_{22}\mu^4 \\
a_{34} &= D_{11}^s\lambda^4 + 2(D_{12}^s + 2D_{66}^s)\lambda^2\,\mu^2 + D_{22}^s\,\mu^4 \\
a_{44} &= H_{11}^s\lambda^4 + 2(H_{11}^s + 2H_{66}^s)\lambda^2\mu^2 + H_{22}^s\mu^4 - A_{55}^s\lambda^2 - A_{44}^s\mu^2
\end{aligned}
\tag{30}
$$

5. Results and discussion

In this study, various examples are presented to illustrate the effect of porosity on the static of two models of FG sandwich plates using the present refined plate theory. The FG plate is taken to be made of aluminum (Al) and zirconia (ZrO_2) with the following material properties:

Ceramic (Zirconia, ZrO_2): $E_c = 151GPa,\ \nu = 0.3.$
Metal (Aluminum, Al): $E_m = 70GPa,\ \nu = 0.3.$
Numerical results are presented in terms of non-dimensional stresses and deflection. The various nondimensional parameters used are

- Central deflection $\overline{W}$: $\overline{W} = \frac{10hE_0}{q_0a^2}W\left(\frac{a}{2},\frac{b}{2}\right)$,
- Axial stress $\overline{\sigma}_x$: $\overline{\sigma}_x = \frac{10.h^2}{q_0a^2}\sigma_x\left(\frac{a}{2},\frac{b}{2},\frac{h}{2}\right)$,
- Shear stress $\overline{\tau}_{xz}$: $\overline{\tau}_{xz} = \frac{h}{q_0a}\tau_{xz}\left(0,\frac{b}{2},0\right)$.

where $E_0 = 1$ GPa. Several kinds of symmetric and non-symmetric FGM sandwich plate are used.

The (1-0-1) FGM sandwich plate: The plate is made of two layers of equal thickness without a core:

$$h_1 = h_2 = 0.$$

The (1-1-1) FGM sandwich plate: The plate is made of three equal-thickness layers:

$$h_1 = -h_2 = h/6.$$

The (1-2-1) FGM sandwich plate: The core thickness equals the sum of faces thickness:

$$h_1 = -h_2 = h/4.$$

The (2-1-2) FGM sandwich plate: The upper layer thickness is twice the core layer while it is the same as the lower one:

$$h_1 = -h_2 = h/10.$$

The (2-2-1) FGM sandwich plate: The core thickness is twice the upper face while it is the same as the lower one

In order to prove the validity of the present refined plate theory, results were obtained for fully FGM plates and compared with the existing ones in the literature (Zenkour 2005) and other theory existing in the literature such as Daikh and Zenkour (2019). Numerical results for the power-law and sigmoid FG sandwich plates are tabulated in Tables 1-3 using the present theory. In addition, our results are compared with those obtained by (Zenkour 2005) using the third-order shear deformation plate theory of Reddy PSDT, the sinusoidal shear deformation plate theory SSDPT and the shape function proposed by Daikh and Zenkour (2019). Table 1 presents the effect volume

Table 1 Effects of volume fraction index on the dimensionless deflection of FGM sandwich plate (*a/h* = 10)

	P	Theories	1-0-1	1-1-1	1-2-1	2-1-2	2-2-1
P-FGM	0	**Present (4 Variables)**	**0.19606**	**0.19606**	**0.19606**	**0.19606**	**0.19606**
		Daikh and Zenkour (2019) (5 variables)	0.19606	0.19606	0.19606	0.19606	0.19606
		TSDPT * (5 variables)	0.19606	0.19606	0.19606	0.19606	0.19606
		SSDPT * (5 variables)	0.19605	0.19605	0.19605	0.19605	0.19605
	1	**Present (4 Variables)**	**0.32358**	**0.29199**	**0.27094**	**0.30631**	**0.28085**
		Daikh and Zenkour (2019) (5 variables)	0.32353	0.29196	0.27094	0.30627	0.28084
		TSDPT * (5 variables)	0.32358	0.29199	0.27094	0.30631	0.28085
		SSDPT * (5 variables)	0.32349	0.29194	0.27093	0.30624	0.28082
	2	**Present (4 Variables)**	**0.37335**	**0.33289**	**0.30263**	**0.35231**	**0.31617**
		Daikh and Zenkour (2019) (5 variables)	0.37326	0.33283	0.30262	0.35224	0.3161
		TSDPT * (5 variables)	0.37335	0.33289	0.30263	0.35231	0.31617
		SSDPT * (5 variables)	0.37319	0.33280	0.30260	0.35218	0.31611
	5	**Present (4 Variables)**	**0.40927**	**0.37145**	**0.33480**	**0.39183**	**0.34960**
		Daikh and Zenkour (2019) (5 variables)	0.40915	0.37136	0.33477	0.39170	0.34954
		TSDPT * (5 variables)	0.40927	0.37145	0.33480	0.39183	0.34960
		SSDPT * (5 variables)	0.40905	0.37128	0.33474	0.39160	0.34950
	10	**Present (4 Variables)**	**0.41772**	**0.38551**	**0.34824**	**0.40407**	**0.36212**
		Daikh and Zenkour (2019) (5 variables)	0.41761	0.38540	0.34819	0.40392	0.36205
		TSDPT * (5 variables)	0.41772	0.38551	0.34824	0.40407	0.36215
		SSDPT * (5 variables)	0.41750	0.38490	0.34119	0.40376	0.34916

Table 1 Continued

	P	Theories	1-0-1	1-1-1	1-2-1	2-1-2	2-2-1
S-FGM FGM	0	**Present (4 Variables)**	**0.267924**	**0.26209**	**0.25377**	**0.26551**	**0.25593**
		Daikh and Zenkour (2019) (5 variables)	0.26791	0.26203	0.25374	0.26546	0.25589
		TSDPT * (5 variables)	0.267924	0.26209	0.25377	0.26551	0.25593
		SSDPT * (5 variables)	0.26790	0.26198	0.25370	0.26540	0.25586
	1	**Present (4 Variables)**	**0.32358**	**0.29199**	**0.27094**	**0.30631**	**0.28085**
		Daikh and Zenkour (2019) (5 variables)	0.32353	0.29196	0.27094	0.30627	0.28084
		TSDPT * (5 variables)	0.32358	0.29199	0.27094	0.30631	0.28085
		SSDPT * (5 variables)	0.32349	0.29194	0.27093	0.30624	0.28082
	2	**Present (4 Variables)**	**0.34171**	**0.30063**	**0.27561**	**0.31871**	**0.28795**
		Daikh and Zenkour (2019) (5 variables)	0.34165	0.30061	0.27562	0.31867	0.28794
		TSDPT * (5 variables)	0.34171	0.30063	0.27561	0.31871	0.28795
		SSDPT * (5 variables)	0.34160	0.30060	0.27562	0.31864	0.28793
	5	**Present (4 Variables)**	**0.35603**	**0.30713**	**0.27906**	**0.32822**	**0.29327**
		Daikh and Zenkour (2019) (5 variables)	0.35597	0.30712	0.27907	0.32819	0.29327
		TSDPT * (5 variables)	0.35603	0.30713	0.27906	0.32822	0.29327
		SSDPT * (5 variables)	0.35591	0.30711	0.27907	0.32817	0.29326
	10	**Present (4 Variables)**	**0.36015**	**0.30895**	**0.28001**	**0.33092**	**0.29476**
		Daikh and Zenkour (2019) (5 variables)	0.36009	0.30895	0.28002	0.33089	0.29475
		TSDPT * (5 variables)	0.36015	0.30895	0.28001	0.33092	0.29476
		SSDPT * (5 variables)	0.36003	0.30894	0.28003	0.33087	0.29475

*Results form Ref. (Zenkour 2005)

Table 2 Effects of volume fraction index on the dimensionless axial stress of FGM sandwich plate (a/h = 5)

	P	Theories	1-0-1	1-1-1	1-2-1	2-1-2	2-2-1
P-FGM	0	**Present (4 Variables)**	**2.04985**	**2.04985**	**2.04985**	**2.04985**	**2.04985**
		Daikh and Zenkour (2019) (5 variables)	2.05248	2.05248	2.05248	2.05248	2.05248
		TSDPT * (5 variables)	2.04985	2.04985	2.04985	2.04985	2.04985
		SSDPT * (5 variables)	2.05452	2.05452	2.05452	2.05452	2.05452
	1	**Present (4 Variables)**	**1.57923**	**1.42617**	**1.32309**	**1.49587**	**1.32062**
		Daikh and Zenkour (2019) (5 variables)	1.58081	1.42771	1.32467	1.49740	1.32219
		TSDPT * (5 variables)	1.57923	1.42617	1.32309	1.49587	1.32062
		SSDPT * (5 variables)	1.58204	1.42892	1.32590	1.49859	1.32342

Table 2 Continued

	P	Theories	1-0-1	1-1-1	1-2-1	2-1-2	2-2-1
P-FGM	2	**Present (4 Variables)**	**1.82167**	**1.62748**	**1.47988**	**1.72144**	**1.47095**
		Daikh and Zenkour (2019) (5 variables)	1.82327	1.62904	1.48153	1.72295	1.47259
		TSDPT * (5 variables)	1.82167	1.62748	1.47988	1.72144	1.47988
		SSDPT * (5 variables)	1.82450	1.63025	1.48283	1.72412	1.48283
	5	**Present (4 Variables)**	**1.99272**	**1.81580**	**1.63814**	**1.91302**	**1.61181**
		Daikh and Zenkour (2019) (5 variables)	1.99439	1.81725	1.63978	1.91441	1.61348
		TSDPT * (5 variables)	1.99272	1.81580	1.63814	1.91302	1.61181
		SSDPT * (5 variables)	1.99567	1.81838	1.64106	1.91547	1.61477
	10	**Present (4 Variables)**	**2.03036**	**1.88377**	**1.70383**	**1.97126**	**1.66479**
		Daikh and Zenkour (2019) (5 variables)	2.03226	1.88515	1.70543	1.97261	1.66646
		TSDPT * (5 variables)	2.03036	1.88376	1.70417	1.97126	1.66660
		SSDPT * (5 variables)	2.03360	1.88147	1.64851	1.97313	1.61979
S-FGM	0	**Present (4 Variables)**	**2.04984**	**2.01169**	**1.94995**	**2.03566**	**1.91770**
		Daikh and Zenkour (2019) (5 variables)	2.05248	2.01367	1.95202	2.03776	1.32219
		TSDPT * (5 variables)	2.04984	2.01169	1.94995	2.03566	1.91770
		SSDPT * (5 variables)	2.05451	2.01518	1.95361	2.03935	1.92165
	1	**Present (4 Variables)**	**1.57923**	**1.42617**	**1.32309**	**1.49587**	**1.32062**
		Daikh and Zenkour (2019) (5 variables)	1.58081	1.42771	1.32467	1.49740	1.32219
		TSDPT * (5 variables)	1.57923	1.42617	1.32309	1.49587	1.32062
		SSDPT * (5 variables)	1.58204	1.42892	1.32590	1.49859	1.32342
	2	**Present (4 Variables)**	**1.66985**	**1.46986**	**1.34697**	**1.55819**	**1.35069**
		Daikh and Zenkour (2019) (5 variables)	1.67142	1.47150	1.34863	1.55980	1.35231
		TSDPT * (5 variables)	1.66985	1.46986	1.34697	1.55819	1.35069
		SSDPT * (5 variables)	1.67263	1.47278	1.34992	1.56105	1.35357
	5	**Present (4 Variables)**	**1.74114**	**1.50267**	**1.36453**	**1.60590**	**1.37315**
		Daikh and Zenkour (2019) (5 variables)	1.74269	1.50439	1.36625	1.60756	1.37481
		TSDPT * (5 variables)	1.74114	1.50267	1.36453	1.60590	1.37315
		SSDPT * (5 variables)	1.74388	1.50573	1.36760	1.60886	1.37610
	10	**Present (4 Variables)**	**1.76160**	**1.51186**	**1.36939**	**1.61939**	**1.37942**
		Daikh and Zenkour (2019) (5 variables)	1.76314	1.51360	1.37113	1.62107	1.38109
		TSDPT * (5 variables)	1.76160	1.51186	1.36939	1.61939	1.37942
		SSDPT * (5 variables)	1.76432	1.51496	1.37249	1.62238	1.38239

Table 3 Effects of volume fraction index on the dimensionless shear stress of FGM sandwich plate (a/h = 10)

	P	Theories	1-0-1	1-1-1	1-2-1	2-1-2	2-2-1
P-FGM	0	**Present (4 Variables)**	**0.23857**	**0.23857**	**0.23857**	**0.23857**	**0.23857**
		Daikh and Zenkour (2019) (5 variables)	0.24278	0.24278	0.24278	0.24278	0.24278
		TSDPT * (5 variables)	0.23857	0.23857	0.23857	0.23857	0.23857
		SSDPT * (5 variables)	0.24618	0.24618	0.24618	0.24618	0.24618
	1	**Present (4 Variables)**	**0.29202**	**0.26116**	**0.25257**	**0.27104**	**0.25950**
		Daikh and Zenkour (2019) (5 variables)	0.29592	0.26498	0.25669	0.27475	0.26353
		TSDPT * (5 variables)	0.29202	0.26116	0.25257	0.27104	0.25950
		SSDPT * (5 variables)	0.29907	0.26809	0.26004	0.27774	0.26680
	2	**Present (4 Variables)**	**0.32622**	**0.27188**	**0.25834**	**0.28838**	**0.26939**
		Daikh and Zenkour (2019) (5 variables)	0.32991	0.27529	0.26224	0.29161	0.27318
		TSDPT * (5 variables)	0.32622	0.27188	0.25834	0.28838	0.26939
		SSDPT * (5 variables)	0.33285	0.27807	0.26543	0.29422	0.27627
	5	**Present (4 Variables)**	**0.38634**	**0.28643**	**0.26512**	**0.31454**	**0.28265**
		Daikh and Zenkour (2019) (5 variables)	0.39046	0.28923	0.26864	0.31720	0.28613
		TSDPT * (5 variables)	0.38634	0.28643	0.26512	0.31454	0.28265
		SSDPT * (5 variables)	0.39370	0.29150	0.27153	0.31930	0.28895
	10	**Present (4 Variables)**	**0.43206**	**0.29566**	**0.26894**	**0.33242**	**0.29083**
		Daikh and Zenkour (2019) (5 variables)	0.43738	0.29817	0.27222	0.33496	0.29420
		TSDPT * (5 variables)	0.43206	0.29529	0.26895	0.33242	0.29080
		SSDPT * (5 variables)	0.44147	0.29566	0.27676	0.33644	0.29671
S-FGM	0	**Present (4 Variables)**	**0.32601**	**0.26966**	**0.25469**	**0.28775**	**0.26691**
		Daikh and Zenkour (2019) (5 variables)	0.33176	0.27318	0.25831	0.29172	0.27083
		TSDPT * (5 variables)	0.32601	0.26966	0.25469	0.28775	0.26691
		SSDPT * (5 variables)	0.33640	0.27599	0.26124	0.29487	0.27399
	1	**Present (4 Variables)**	**0.29202**	**0.26116**	**0.25257**	**0.27104**	**0.25950**
		Daikh and Zenkour (2019) (5 variables)	0.29592	0.26498	0.25669	0.27475	0.26353
		TSDPT * (5 variables)	0.29202	0.26116	0.25257	0.27104	0.25950
		SSDPT * (5 variables)	0.29907	0.26809	0.26004	0.27774	0.26680
	2	**Present (4 Variables)**	**0.28377**	**0.25908**	**0.25207**	**0.26696**	**0.25762**
		Daikh and Zenkour (2019) (5 variables)	0.28725	0.26300	0.25631	0.27063	0.26168
		TSDPT * (5 variables)	0.28377	0.25908	0.25207	0.26696	0.25762
		SSDPT * (5 variables)	0.29005	0.26620	0.25978	0.27361	0.26498

Table 3 Continued

	P	Theories	1-0-1	1-1-1	1-2-1	2-1-2	2-2-1
S-FGM	5	**Present (4 Variables)**	**0.27751**	**0.25753**	**0.25168**	**0.26389**	**0.25617**
		Daikh and Zenkour (2019) (5 variables)	0.28065	0.26152	0.25603	0.26753	0.26026
		TSDPT * (5 variables)	0.27751	0.25753	0.25168	0.26389	0.25617
		SSDPT * (5 variables)	0.28321	0.26480	0.25959	0.27051	0.26360
	10	**Present (4 Variables)**	**0.27568**	**0.25707**	**0.25156**	**0.26299**	**0.25575**
		Daikh and Zenkour (2019) (5 variables)	0.27871	0.26109	0.25595	0.26663	0.25985
		TSDPT * (5 variables)	0.27568	0.25707	0.25156	0.26299	0.25575
		SSDPT * (5 variables)	0.28119	0.26439	0.25953	0.26961	0.26319

fraction index p on the central deflections of P and S-FGM sandwich plates. The deflections increase as the volume fraction index increase. Axial and shear stresses for different values of index p are depicted in Tables 2 and 3, respectively. Also, it is found that the present results are in good agreement with various shear deformation theories provided by Zenkour (2005) and the theory proposed by Daikh and Zenkour (2019). The influence of porosities distribution on the deflections of P-FGM and S-FGM sandwich plates for side-to-thickness $a/h = 10$ and volume fraction index $p = 2$ is depicted in Table 4. The porosity coefficient is chosen as $\alpha = 0.1,0.2$. It is clear that the deflection obtained for perfect plates $(\alpha = 0)$ is smaller than that for $\alpha = 0.1$and the latter is smaller than that for $\alpha = 0.2$.

Table 4 Effects of porosity on the dimensionless deflection of the FGM square sandwich plate (a/h = 10, p = 2)

	Sheme	Theories	Perfect $\alpha = 0$	Imperfect I		Imperfect II		Imperfect III		Imperfect IV	
				$\alpha = 0.1$	$\alpha = 0.2$	$\alpha = 0.1$	$\alpha = 0.2$	$\alpha = 0.1$	$\alpha = 0.2$	$\alpha = 0.1$	$\alpha = 0.2$
P-FGM	1-0-1	**Present**	**0.37334**	**0.44162**	**0.53570**	**0.40082**	**0.43172**	**0.40011**	**0.42866**	**0.38915**	**0.40606**
		Daikh and Zenkour (2019)	0.37326	0.44152	0.53558	0.40071	0.43159	0.40001	0.42853	0.38970	0.40596
		TSDPT *	0.37334	0.44162	0.53570	0.40082	0.43172	0.40011	0.42866	0.38915	0.40606
		SSDPT *	0.37319	0.44143	0.53547	0.40062	0.43147	0.39991	0.42841	0.38898	0.40587
	1-1-1	**Present**	**0.33288**	**0.38414**	**0.45086**	**0.35590**	**0.38155**	**0.35531**	**0.37901**	**0.34951**	**0.36741**
		Daikh and Zenkour (2019)	0.33283	0.38408	0.45079	0.35584	0.38148	0.35526	0.37895	0.34946	0.36734
		TSDPT *	0.33288	0.38414	0.45086	0.35590	0.38155	0.35531	0.37901	0.34951	0.36741
		SSDPT *	0.33280	0.38403	0.45074	0.35579	0.38142	0.35521	0.37889	0.34940	0.36728
	1-2-1	**Present**	**0.30262**	**0.34013**	**0.38608**	**0.32007**	**0.33906**	**0.31963**	**0.33720**	**0.31672**	**0.33176**
		Daikh and Zenkour (2019)	0.30262	0.34012	0.38606	0.32005	0.33904	0.31961	0.33719	0.31671	0.33174
		TSDPT *	0.30262	0.34013	0.38608	0.32007	0.33906	0.31963	0.33720	0.31672	0.33176
		SSDPT *	0.30260	0.34010	0.38605	0.32004	0.33903	0.31960	0.33717	0.31669	0.33171

Table 4 Continued

	Sheme	Theories	Perfect $\alpha = 0$	Imperfect I		Imperfect II		Imperfect III		Imperfect IV	
				$\alpha = 0.1$	$\alpha = 0.2$	$\alpha = 0.1$	$\alpha = 0.2$	$\alpha = 0.1$	$\alpha = 0.2$	$\alpha = 0.1$	$\alpha = 0.2$
P-FGM	2-1-2	**Present**	**0.35231**	**0.41216**	**0.49258**	**0.37825**	**0.40743**	**0.37759**	**0.40453**	**0.36931**	**0.38760**
		Daikh and Zenkour (2019)	0.35224	0.41208	0.49248	0.37817	0.40732	0.37750	0.40443	0.36927	0.38750
		TSDPT *	0.35231	0.41216	0.49258	0.37825	0.40743	0.37759	0.40453	0.36931	0.38760
		SSDPT *	0.35218	0.41200	0.49239	0.37809	0.40723	0.37743	0.40434	0.36916	0.38741
	2-2-1	**Present**	**0.31616**	**0.35966**	**0.41504**	**0.33579**	**0.35745**	**0.33529**	**0.35532**	**0.33071**	**0.34627**
		Daikh and Zenkour (2019)	0.31614	0.35963	0.41501	0.33575	0.35741	0.33525	0.35528	0.33069	0.34623
		TSDPT *	0.31616	0.35966	0.41504	0.33579	0.35745	0.33529	0.35532	0.33071	0.34627
		SSDPT *	0.31611	0.35960	0.41498	0.33572	0.35737	0.33522	0.35524	0.33064	0.34619
S-FGM	1-0-1	**Present**	**0.34171**	**0.39880**	**0.47490**	**0.36502**	**0.39092**	**0.36443**	**0.38837**	**0.35512**	**0.36935**
		Daikh and Zenkour (2019)	0.34165	0.39874	0.47483	0.36495	0.39084	0.36436	0.38828	0.35506	0.36929
		TSDPT *	0.34171	0.39880	0.47490	0.36502	0.39092	0.36443	0.38837	0.35512	0.36935
		SSDPT *	0.34160	0.39868	0.47477	0.36489	0.39076	0.36429	0.38821	0.35501	0.36923
	1-1-1	**Present**	**0.30063**	**0.34233**	**0.39488**	**0.31961**	**0.34048**	**0.31913**	**0.33843**	**0.31440**	**0.32908**
		Daikh and Zenkour (2019)	0.30061	0.34231	0.39486	0.31959	0.34045	0.31911	0.33841	0.31438	0.32905
		TSDPT *	0.30063	0.34233	0.39488	0.31961	0.34048	0.31913	0.33843	0.31440	0.32908
		SSDPT *	0.30060	0.34229	0.39483	0.31957	0.34042	0.31909	0.33838	0.31435	0.32902
	1-2-1	**Present**	**0.27561**	**0.30677**	**0.34405**	**0.29027**	**0.30605**	**0.28990**	**0.30452**	**0.28749**	**0.30004**
		Daikh and Zenkour (2019)	0.27562	0.30677	0.34406	0.29027	0.30605	0.28990	0.30452	0.28749	0.30004
		TSDPT *	0.27561	0.30677	0.34405	0.29027	0.30605	0.28990	0.30452	0.28749	0.30004
		SSDPT *	0.27562	0.30677	0.34406	0.29027	0.30605	0.28990	0.30452	0.28748	0.30003
	2-1-2	**Present**	**0.31871**	**0.36752**	**0.43085**	**0.34018**	**0.36400**	**0.33964**	**0.36165**	**0.33285**	**0.34791**
		Daikh and Zenkour (2019)	0.31867	0.36749	0.43080	0.34014	0.36394	0.33959	0.36160	0.33281	0.34786
		TSDPT *	0.31871	0.36752	0.43085	0.34018	0.36400	0.33964	0.36165	0.33285	0.34791
		SSDPT *	0.31864	0.36745	0.43076	0.340104	0.36389	0.33955	0.36155	0.33277	0.34782
	2-2-1	**Present**	**0.28795**	**0.32379**	**0.36808**	**0.30432**	**0.32217**	**0.30391**	**0.32043**	**0.30015**	**0.31307**
		Daikh and Zenkour (2019)	0.28794	0.32378	0.36807	0.30431	0.32216	0.30390	0.32041	0.30013	0.31306
		TSDPT *	0.28795	0.32379	0.36808	0.30432	0.32217	0.30391	0.32043	0.30015	0.31307
		SSDPT *	0.28793	0.32377	0.36806	0.30430	0.32214	0.30388	0.32040	0.30012	0.31304

The major problem in sandwich structures is the abrupt change in material properties across the interfaces between the face layers and the core, the continuously and smoothly varying material

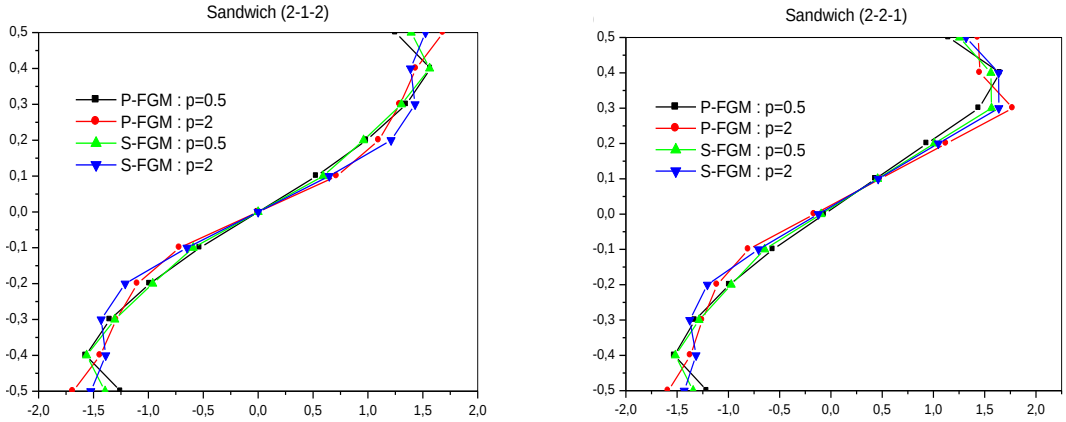

Fig. 2 Dimensionless axial stress through-the-thickness of FGM sandwich plate

properties of FGM help to eliminate this problem due to proficient and continuous change of material properties at the interfaces.

A comparison study of non-dimensional stresses in P-FGM and S-FGM sandwich plates is reported in Figs. 2 and 3 with various FGM sandwich schemes. The volume fraction index is chosen as $p = 0.5, 2$. It is clear that axial and shear stresses in P-FGM sandwich with index $p = 0.5$, and S-FGM sandwich with index $p = 2$ are continuous and smooth through the plate sandwich thickness, but non-smooth at the interfaces for P-FGM with index $p = 2$ and S-FGM sandwich with index $p = 0.5$. The axial stresses $\overline{\sigma}_{xx}$ are tensile at the top surface and compressive at the bottom surface (Fig. 2). From Fig. 3, the maximum values of the shear stress occur at a point on the mid-plane of the plate wherever the FGM sandwich scheme is.

Fig. 4 shows the variation of the center deflection $\overline{w}$ with the side-to-thickness ratio for different schemes of FGM sandwich plates. It can be observed that the deflection of the sandwich plate (1-0-1) is found to be the largest magnitude, and as the side-to-thickness increases the deflection will increase. Also, the deflections of the sandwich S-FGM are smaller than that of P-FGM sandwich plates.

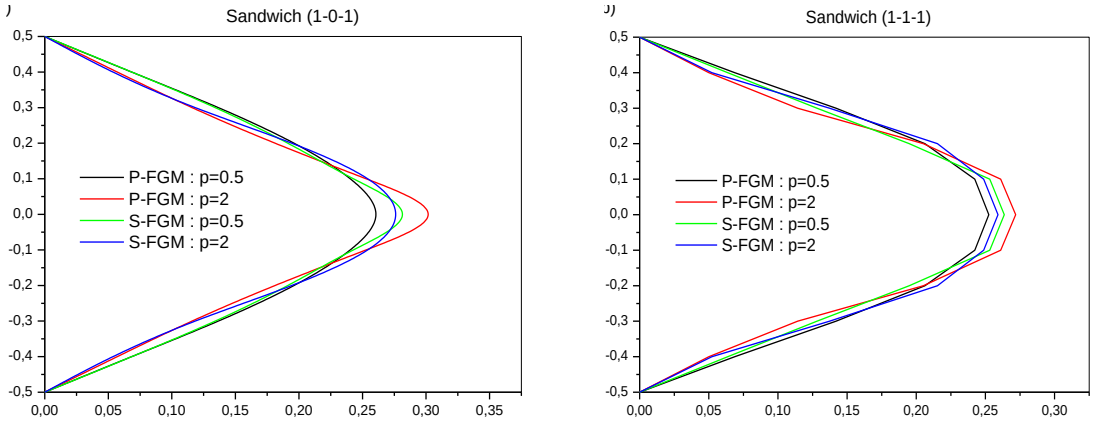

Fig. 3 Dimensionless shear stress through-the-thickness of FGM sandwich plate

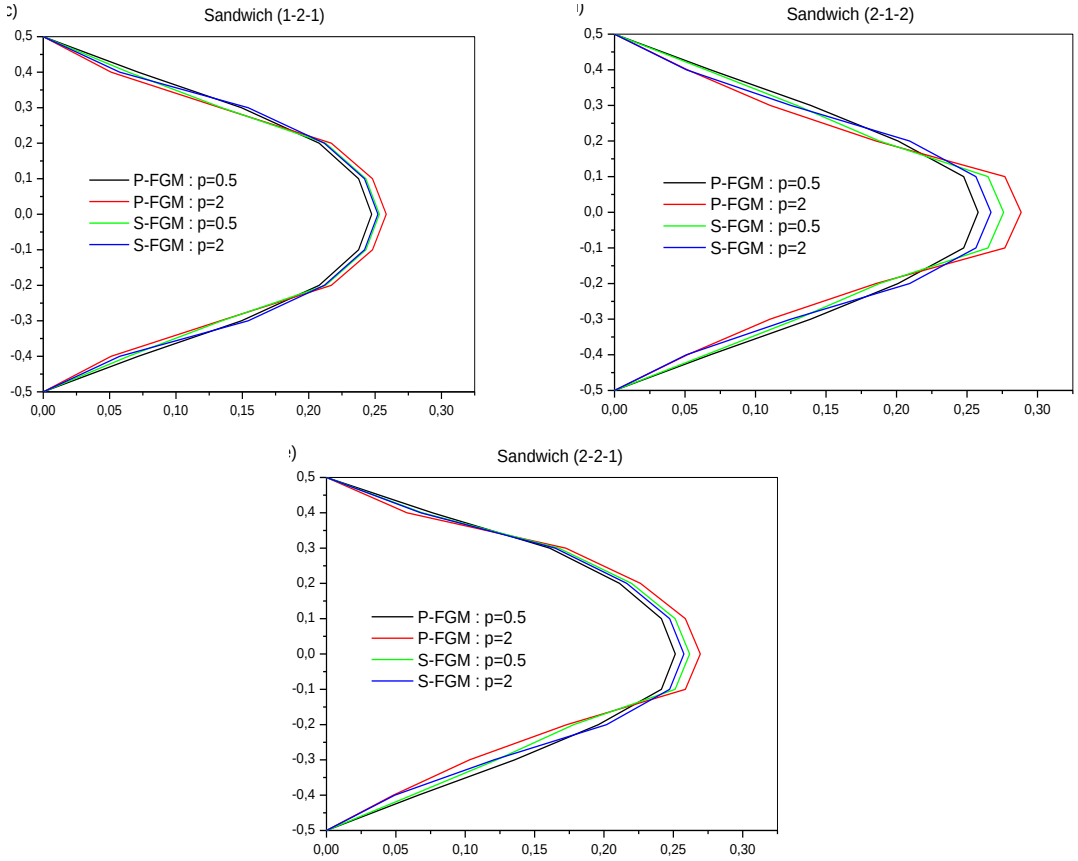

Fig. 3 Continued

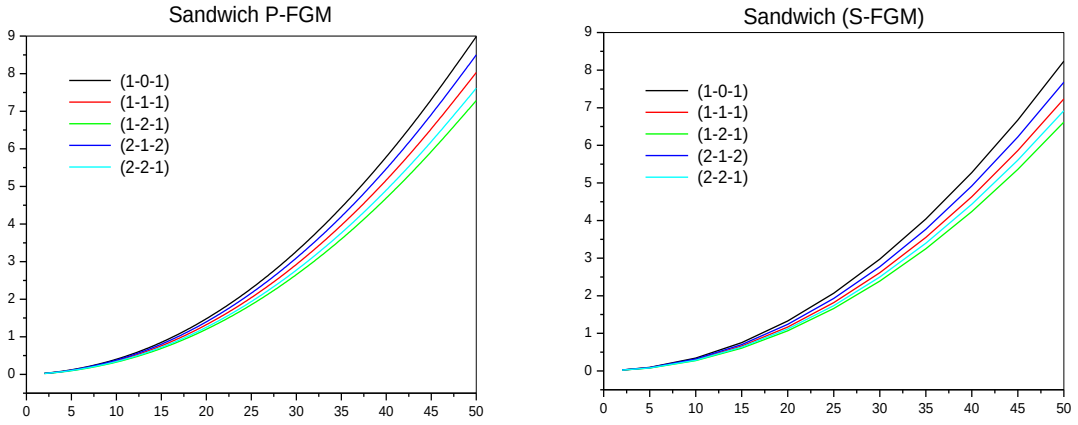

Fig. 4 Dimensionless center deflection of FGM sandwich plate versus side-to-thickness a/h $(p = 2)$

Fig. 5 indicates the effect the side-to-thickness ratio and the porosity models on the center deflections of (2-1-2) sandwich plates with volume fraction $p = 2$ and porosity coefficient $\alpha =$

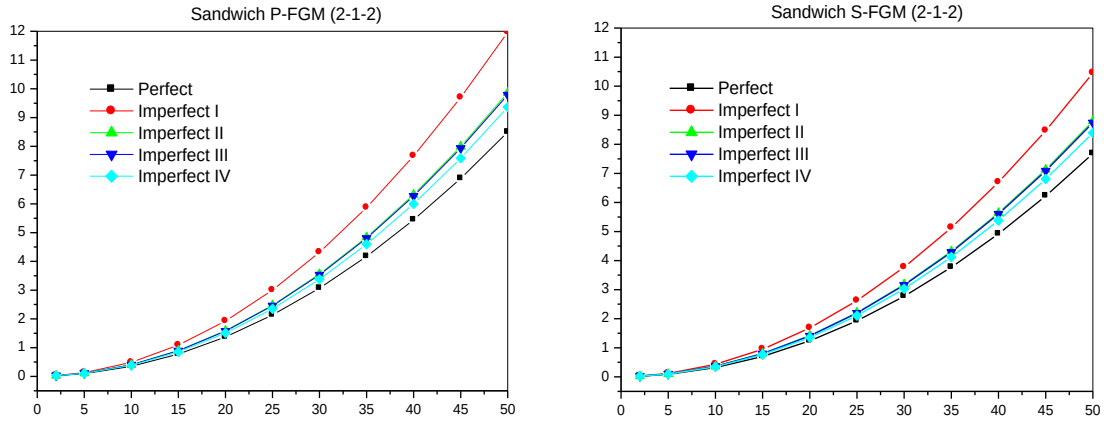

Fig. 5 Dimensionless center deflection of FGM sandwich plate versus side-to-thickness a/h $(p = 2)$

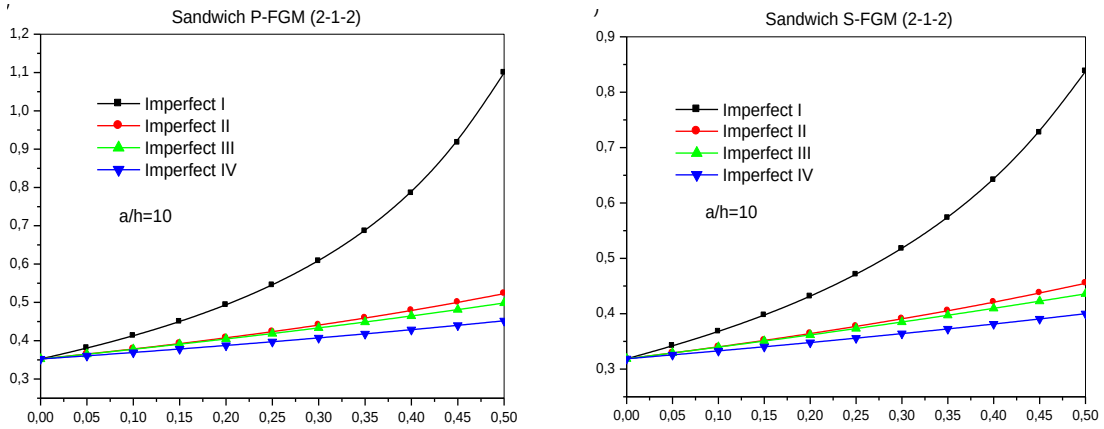

Fig. 6 Effect of porosity coefficient on center deflection FGM sandwich plate (2-1-2) $(p = 2)$

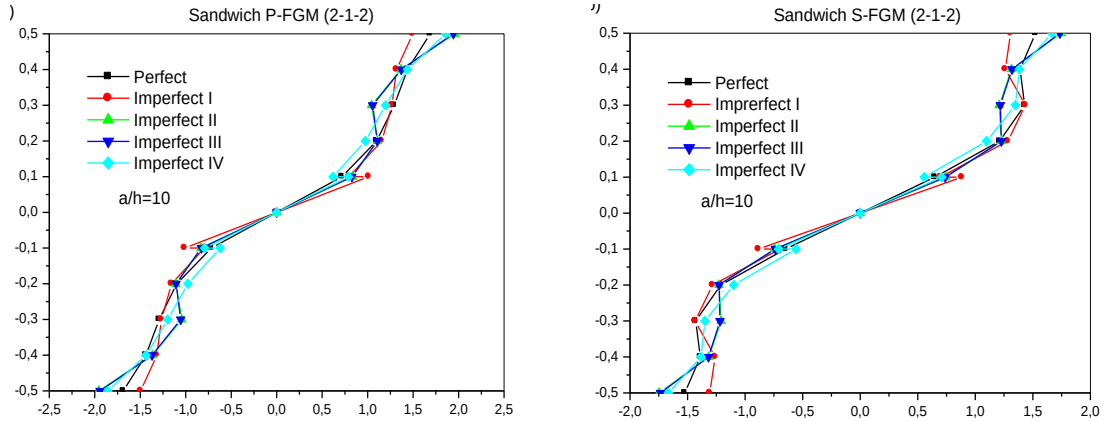

Fig. 7 Effect of porosity coefficient on dimensionless axial stress FGM sandwich plate (2-1-2) $(p = 2)$

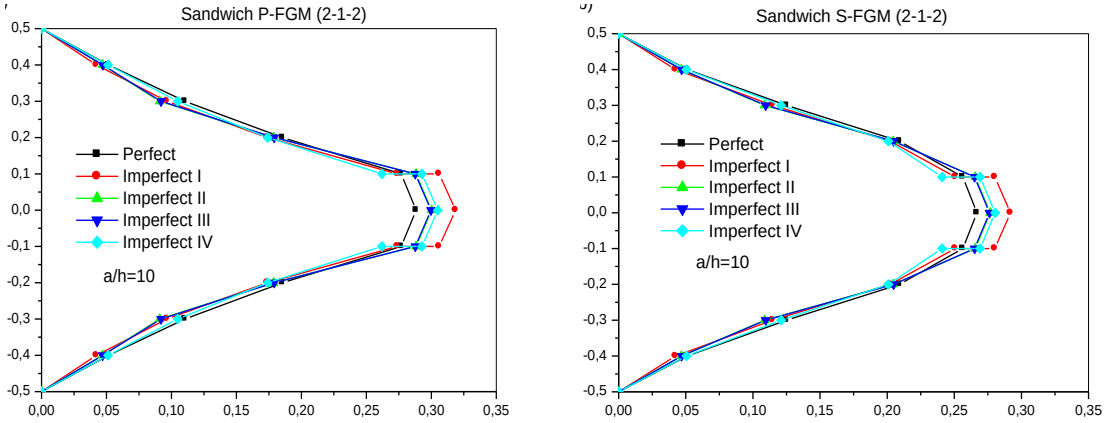

Fig. 8 Effect of porosity coefficient on dimensionless shear stress FGM sandwich plate (2-1-2) $(p = 2)$

0.2. The deflections for plate with uniform porosity distribution model (Imperfect I) are higher than that for the other models of imperfect FGM sandwich plates. It is clear that the difference between perfect and imperfect sandwich plates increase with increasing of side-to-thickness ratio.

Variation of porosity coefficient α on the central deflection is illustrated in Fig. 6. The porosity coefficient has an important effect on the defluxions mainly for even distribution model (Imperfect I) where the increasing of porosity coefficient increases the central deflections.

Figs. 7 and 8 show the effect of porosity coefficient α on the axial stress and shear stress, respectively. The axial stress and shear stress are continuous and smooth through the plate sandwich thickness for Perfect, Imperfect II and Imperfect III FGM sandwich plates and non-smooth for Imperfect I and Imperfect IV.

6. Conclusions

A four variable refined theory is extended to the bending response of rectangular FGM sandwich plates with new definition of porosity distribution taking into account composition and the scheme of the sandwich plate. The number of primary variables in this theory is even less than that of first- and higher-order shear deformation plate theories. Hence, unlike any other theory, the theory presented gives rise to only four governing equations resulting in considerably lower computational effort when compared with the other higher-order theories reported in the literature having more number of governing equations. The theory accounts for parabolic distribution of the transverse shear strains through the plate thickness, and satisfies the zero traction boundary conditions on the surfaces of the plate without using shear correction factors. The accuracy and efficiency of the present theory has been demonstrated for bending behaviors of simply supported FGM sandwich plates. In general, the power-law is used to define the volume fraction of the FGM sandwich. In this paper, for the first time, bending of FG sandwich plates based on power-law and sigmoid function with porous FGM layers is presented. Four models of porosity distribution are proposed. As a result, the deflections are minimums for non-porous FGM sandwich plates and increase when the porosity coefficient increase regardless the porosity type. The increasing of side-to-thickness ratio increase the central deflections.

References

Ait Yahia, S., Ait Atmane, H., Houari, M.S.A. and Tounsi, A. (2015), "Wave propagation in functionally graded plates with porosities using various higher-order shear deformation plate theories", *Struct. Eng. Mech., Int. J.*, **53**(6), 1143-1165. https://doi.org/10.12989/sem.2015.53.6.1143

Akbaş, S.D. (2015a), "Wave propagation of a functionally graded beam in thermal environments", *Steel Compos. Struct., Int. J.*, **19**(6), 1421-1447. https://doi.org/10.12989/scs.2015.19.6.1421

Akbaş, S.D. (2015b), "Post-buckling analysis of axially functionally graded three-dimensional beams", *Int. J. Appl. Mech.*, **7**(3), 1550047. https://doi.org/10.1142/S1758825115500477

Akbaş, S.D. (2017a), "Free vibration of edge cracked functionally graded microscale beams based on the modified couple stress theory", *Int. J. Struct. Stabil. Dyn.*, **17**(3), 1750033. https://doi.org/10.1142/S021945541750033X

Akbaş, S.D. (2017b), "Thermal effects on the vibration of functionally graded deep beams with porosity", *Int. J. Appl. Mech.*, **9**(5), 1750076. https://doi.org/10.1142/S1758825117500764

Akbaş, S.D. (2017c), "Forced vibration analysis of functionally graded nanobeams", *Int. J. Appl. Mech.*, **9**(7), 1750100. https://doi.org/10.1142/S1758825117501009

Akbaş, S.D. (2018a), "Nonlinear thermal displacements of laminated composite beams", *Coupl. Syst. Mech., Int. J.*, **7**(6), 691-705. https://doi.org/10.12989/csm.2018.7.6.691

Akbaş, S.D. (2018b), "Forced vibration analysis of cracked nanobeams", *J. Brazil. Soc. Mech. Sci. Eng.*, **40**(8), 392. https://doi.org/10.1007/s40430-018-1315-1

Akbaş, S.D. (2018c), "Forced vibration analysis of cracked functionally graded microbeams", *Adv. Nano Res., Int. J.*, **6**(1), 39-55. https://doi.org/10.12989/anr.2018.6.1.039

Benhenni, M.A., Hassaine Daouadji, T., Abbes, B., Adim, B., Li, Y. and Abbes, F. (2018), "Dynamic analysis for anti-symmetric cross-ply and angle-ply laminates for simply supported thick hybrid rectangular plates", *Adv. Mater. Res., Int. J.*, **7**(2), 119-136. https://doi.org/10.12989/amr.2018.7.2.119

Bourada, F., Bousahla, A.A., Bourada, M., Azzaz, A., Zinata, A. and Tounsi, A. (2019), "Dynamic investigation of porous functionally graded beam using a sinusoidal shear deformation theory", *Wind Struct., Int. J.*, **28**(1), 19-30. https://doi.org/10.12989/was.2019.28.1.019

Daikh, A.A. and Zenkour, A.M. (2019), "Effect of porosity on the bending analysis of various functionally graded sandwich plates", *Mater. Res. Express*, **6**(6), 065703. https://doi.org/10.1088/2053-1591/ab0971

Hellal, H., Bourada, M., Hebali, H., Bourada, F., Tounsi, A., Bousahla, A.A. and Mahmoud, S.R. (2019), "Dynamic and stability analysis of functionally graded material sandwich plates in hygro-thermal environment using a simple higher shear deformation theory", *J. Sandw. Struct. Mater.* https://doi.org/10.1177/1099636219845841

Kadoli, R., Akhtar, K. and Ganesan, N. (2008), "Static analysis of functionally graded beams using higher order shear deformation theory", *Appl. Math. Model.*, **32**(12), 2509-2525. https://doi.org/10.1016/j.apm.2007.09.015

Karamanlı, A. (2017), "Bending behaviour of two directional functionally graded sandwich beams by using a quasi-3d shear deformation theory", *Compos. Struct.*, **174**, 70-86. https://doi.org/10.1016/j.compstruct.2017.04.046

Meksi, R., Benyoucef, S., Mahmoudi, A., Tounsi, A., Adda Bedia, E.A. and Mahmoud, S.R. (2019), "An analytical solution for bending, buckling and vibration responses of FGM sandwich plates", *J. Sandw. Struct. Mater.*, **21**(2), 727-757. https://doi.org/10.1177/1099636217698443

Menaa, R., Tounsi, A., Mouaici, F., Mechab, I., Zidi, M. and Adda Bedia, E.A. (2012), "Analytical solutions for static shear correction factor of functionally graded rectangular beams", *Mech. Adv. Mater. Struct.*, **19**, 641-652. https://doi.org/10.1080/15376494.2011.581409

Safa, A., Hadji, L. and Bourada, M. (2019), "Thermal vibration analysis of FGM beams using an efficient shear deformation beam theory", *Earthq. Struct., Int. J.*, **17**(3), 329-336. https://doi.org/10.12989/eas.2019.17.3.329

Sahouane, A., Hadji, L. and Bourada, M. (2019), "Numerical analysis for free vibration of functionally

graded beams using an original HSDBT", *Earthq. Struct., Int. J.*, **17**(1), 31-37. https://doi.org/10.12989/eas.2019.17.1.031

Shashank, P. and Pradyumna, S. (2018), "Analysis of functionally graded sandwich plates using a higher-order layerwise theory", *Compos. Part B*, **153**, 325-336. https://doi.org/10.1016/j.compositesb.2018.08.121

Simsek, M. (2010), "Fundamental frequency analysis of functionally graded beams by using different higher-order beam theories", *Nuc. Eng. Des.*, **240**, 697-705. https://doi.org/10.1016/j.nucengdes.2009.12.013

Simsek, M. and Al-shujairi, M. (2017), "Static, free and forced vibration of functionally graded (FG) sandwich beams excited by two successive moving harmonic loads", *Compos. Part B*, **108**, 18-34. https://doi.org/10.1016/j.compositesb.2016.09.098

Tounsi, A., Houari, M.S.A. and Benyoucef, S. (2013), "A refined trigonometric shear deformation theory for thermoelastic bending of functionally graded sandwich plates", *Aerosp. Sci. Technol.*, **24**, 209-220. https://doi.org/10.1016/j.ast.2011.11.009

Vo, T.P., Thai, H.T., Nguyen, T.K., Inam, F. and Lee, J. (2015), "Static behaviour of functionally graded sandwich beams using a quasi-3D theory", *Compos.: Part B*, **68**, 59-74. https://doi.org/10.1016/j.compositesb.2014.08.030

Wattanasakulpong, N. and Ungbhakorn, V. (2014), "Linear and nonlinear vibration analysis of elastically restrained ends FGM beams with porosities", *Aerosp. Sci. Technol.*, **32**(1), 111-120. https://doi.org/10.1016/j.ast.2013.12.002

Wattanasakulpong, N., Prusty, B.G., Kelly, D.W. and Hoffman, M. (2012), "Free vibration analysis of layered functionally graded beams with experimental validation", *Mater. Des.*, **36**, 182-190. https://doi.org/10.1016/j.matdes.2011.10.049

Xuan, H.N., Thai, C.H. and Thoi, T.N. (2013), "Isogeometric finite element analysis of composite sandwich plates using a higher order shear deformation theory", *Compos.: Part B*, **55**, 558-574. https://doi.org/10.1016/j.compositesb.2013.06.044

Zarga, D., Tounsi, A., Bousahla, A.A., Bourada, F. and Mahmoud, S.R. (2019), "Thermomechanical bending study for functionally graded sandwich plates using a simple quasi-3D shear deformation theory", *Steel Compos. Struct., Int. J.*, **32**(3), 389-410. https://doi.org/10.12989/scs.2019.32.3.389

Zenkour, A.M. (2005), "A comprehensive analysis of functionally graded sandwich plates: Part 1—Deflection and stresses", *Int. J. Solids Struct.*, **42**, 5224-5242. https://doi.org/10.1016/j.ijsolstr.2005.02.015

Zenkour, A.M. and Alghamdi, N. (2010), "Bending analysis of functionally graded sandwich plates under the effect of mechanical and thermal loads", *Mech. Adv. Mater. Struct.*, **17**, 419-432. https://doi.org/10.1080/15376494.2010.483323

Zouatnia, N. and Hadji, L. (2019), "Effect of the micromechanical models on the bending of FGM beam using a new hyperbolic shear deformation theory", *Earthq. Struct., Int. J.*, **16**(2), 177-183. https://doi.org/10.12989/eas.2019.16.2.177

Zhu, J., Lai, Z., Yin, Z., Jeon, J. and Lee, S. (2001), "Fabrication of ZrO_2–NiCr functionally graded material by powder metallurgy", *Mater. Chem. Phys.*, **68**, 130-135. https://doi.org/10.1016/S0254-0584(00)00355-2

CC